

PAPER • OPEN ACCESS

Design of controllers for omnidirectional robot based on the system identification technique for trajectory tracking

To cite this article: A N Amudhan *et al* 2019 *J. Phys.: Conf. Ser.* **1240** 012146

View the [article online](#) for updates and enhancements.

You may also like

- [Trajectory Tracking Control of the Wheeled Mobile Robot based on the Curve Tracking Algorithm](#)
Youhua Peng, Peng Zhang, Zheng Fang et al.
- [Sliding Mode Control for Trajectory Tracking of AGV Based on Improved Fast Stationary Power Approach Law](#)
Xiaorong Zhou and Lin He
- [A Sliding mode control method for trajectory tracking control of wheeled mobile robot](#)
Lu Yang and Shenghui Pan



PRIME
PACIFIC RIM MEETING
ON ELECTROCHEMICAL
AND SOLID STATE SCIENCE

HONOLULU, HI
Oct 6–11, 2024

Abstract submission deadline:
April 12, 2024

Learn more and submit!



Joint Meeting of

The Electrochemical Society
•
The Electrochemical Society of Japan
•
Korea Electrochemical Society



Design of controllers for omnidirectional robot based on the system identification technique for trajectory tracking

A N Amudhan¹, P Sakthivel², A P Sudheer^{1,3} and T K Sunil Kumar²

¹Department of Mechanical Engineering, National Institute of Technology Calicut, India

²Department of Electrical Engineering, National Institute of Technology Calicut, India

³apsudheer@nitc.ac.in

Abstract:

Omnidirectional wheeled mobile robots are gaining a lot of importance owing to its widespread applications in healthcare, industries and various other service sectors. Most of these applications demand the mobile base to track the desired trajectory with the desired speed, optimal time and energy consumption. This work focusses on the trajectory tracking of the four-wheeled mobile robot with omnidirectional wheels. Most of the existing works make use of the models developed using first principles but in this work, system modeling is carried out by the system identification technique using the data obtained from the fabricated mobile base. Trajectory tracking is then carried out using PID and Linear Quadratic Tracking (LQT) based controllers. The simulation results are compared for tracking errors and energy consumption and the results obtained in real time are presented.

1. Introduction:

Wheel based mobile robots prove to be a potential area of research for decades. With the advancements of technology in various domains, the use of mobile robots finds numerous applications and hence remains to be the area of interest to researchers, students and industrialists. The common areas of application include various service sectors such as in hospitals, banking, museums, process control, defense, navigation and various surveillance applications. In industries, mobile manipulators prove to be more useful than the commonly found stationary manipulators [1]. Thus, these wheeled mobile robots(WMR) is integrated with various system that suits the respective application and are of use in various manufacturing and service sectors. Therefore, the studies on navigation, path planning, obstacle avoidance, trajectory tracking of the WMR are useful for various applications [2].

Most commonly found WMR are the differential drive mobile robots with two standard wheels. Extensive works are carried out on the design and control of two wheeled mobile robots [3-5]. One disadvantage of these two wheeled mobile robot is that they do not allow motion in the lateral direction which is overcome by the use of the omnidirectional mobile robots. The movement in lateral direction is more advantageous in cluttered environments where the mobile base suffers from space constraint for its angular rotation. Numerous methods are adopted to achieve such omnidirectional mobility. The typical method of obtaining such omnidirectional motion is by using omnidirectional wheels [6] and meccanum wheels [7]. These are special type of wheels that contain rollers along its



periphery. Other methods include the use of spherical wheels [8,9], ball wheels [10] and other special type of attachments with the mobile base to achieve omnidirectional motion. Substantial works are done on the design of trajectory tracking controller for mobile robots that includes fuzzy [11], back stepping method [12], robust [13], PID [14], sliding mode controllers and much more but most of these work make use of the dynamic model developed using Euler-lagrangian, or simple force analysis there by incorporating actuator dynamics and Coriolis forces. In this work, four-wheeled omnidirectional robots are considered whose modeling is done using system identification technique. The trajectory tracking of the system is done using the optimal LQR controller and the results are compared with the PI controller.

Section II of the paper briefs on Kinematic modelling of the mobile base; Section III deals with the development of the model using system identification technique and details on the advantage of using this technique; Section IV deals with the controller design of the model developed using system identification technique; and Section V details on the results of the designed controller and section VI concludes the work stating its future scope.

2. DEVELOPMENT OF THE KINEMATIC MODEL

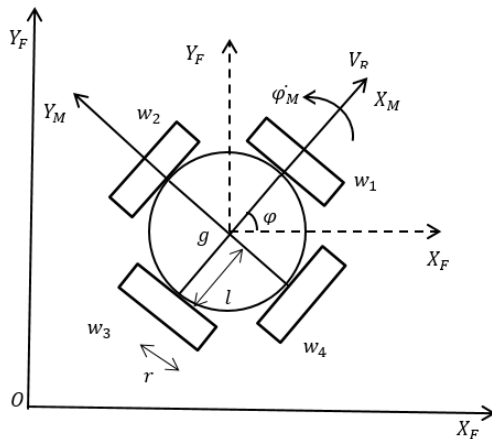


Figure 1. Structure of the robot.

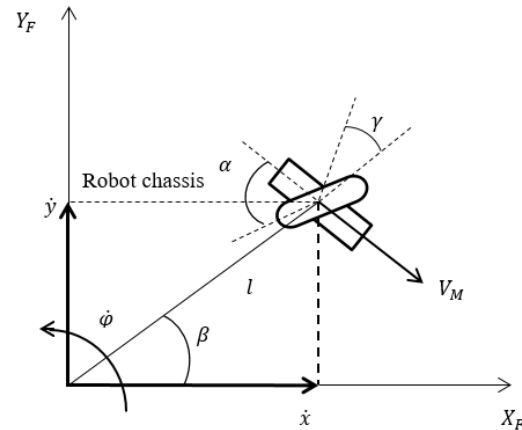


Figure 2. Velocity vector analysis of a single wheel.

The kinematic model helps in the accurate positioning and orienting of the robot. In the case of robot manipulators, the forward kinematic model gives the position of the end effector in terms of joint angles where as in the case of mobile robots, position and orientation of the mobile robot is based on the velocities of each wheel. Hence, it is referred as forward differential kinematics which relates the linear and angular velocities of the robot as a function of wheel velocities. Figure 1 represents the schematic of the four omnidirectional-wheeled mobile robot.

Two frames are considered for the development of the kinematic model: fixed frame $X_F Y_F$ and moving frame $X_M Y_M$. ϕ is angle between the two frames and is also the heading angle of the robot on the fixed frame. The fixed frame and the moving frame are related according to the following expression,

$$\dot{\xi}_M = R(\phi) \dot{\xi}_F \quad (1)$$

Figure 2 shows the parameters involved in the velocity vector analysis of a single wheel. Here, l refers to the distance of the wheel to the center of gravity of the robot (g), γ refers to the steering angle of the wheel, β is the angle between the line joining the wheel with ' g ' and the robot's x-axis (X_M), α represents the angle made by the roller's axis and the wheel plane. The input to the system is the

velocity induced in the wheels due to the voltage applied. This velocity is expressed as three components along \dot{x} , \dot{y} and $\dot{\varphi}$ in the robot(moving) frame which gives:

$$[\sin(\beta + \gamma) \quad -\cos(\beta + \gamma) \quad -l \cos(\gamma)] \dot{\xi}_M - r \dot{\theta} \cos \alpha = 0 \quad (2)$$

where r is the radius of the wheel and $\dot{\theta}$ is the angular velocity of the wheel. The angle $\alpha = 0$ in the case of omnidirectional wheels since the axis of the rollers align with the wheel plane.

Upon substituting eqn (1) in (2) and extending the same to all the four wheels yields,

$$\dot{\xi}_I = [J]^{-1} [R(\varphi)]^{-1} r \dot{\theta} \quad (3)$$

$$\text{where, } J = \begin{bmatrix} \sin(\beta_1 + \gamma_1) & -\cos(\beta_1 + \gamma_1) & -l_1 \cos(\gamma_1) \\ \sin(\beta_2 + \gamma_2) & -\cos(\beta_2 + \gamma_2) & -l_2 \cos(\gamma_2) \\ \sin(\beta_3 + \gamma_3) & -\cos(\beta_3 + \gamma_3) & -l_3 \cos(\gamma_3) \\ \sin(\beta_4 + \gamma_4) & -\cos(\beta_4 + \gamma_4) & -l_4 \cos(\gamma_4) \end{bmatrix}; \text{ and } R(\varphi) = \begin{bmatrix} \cos \varphi & \sin \varphi & 0 \\ -\sin \varphi & \cos \varphi & 0 \\ 0 & 0 & 1 \end{bmatrix}$$

$$\dot{\theta} = [\dot{\theta}_1 \quad \dot{\theta}_2 \quad \dot{\theta}_3 \quad \dot{\theta}_4]^T$$

Values for various parameters for the configuration shown in fig. 1 are,

$$\beta_1 = 0^\circ; \beta_2 = 90^\circ; \beta_3 = 180^\circ; \beta_4 = 270^\circ; \gamma_1 = \gamma_2 = \gamma_3 = \gamma_4 = 0^\circ; l_1 = l_2 = l_3 = l_4 = l;$$

Substituting the above values results in the forward differential kinematics as follows,

$$\begin{bmatrix} \dot{x} \\ \dot{y} \\ \dot{\varphi} \end{bmatrix} = \begin{bmatrix} \frac{r}{2} \sin \varphi & \frac{r}{2} \cos \varphi & -\frac{r}{2} \sin \varphi & -\frac{r}{2} \cos \varphi \\ -\frac{r}{2} \cos \varphi & \frac{r}{2} \sin \varphi & \frac{r}{2} \cos \varphi & -\frac{r}{2} \sin \varphi \\ -\frac{r}{4l} & -\frac{r}{4l} & -\frac{r}{4l} & -\frac{r}{4l} \end{bmatrix} \begin{bmatrix} \dot{\theta}_1 \\ \dot{\theta}_2 \\ \dot{\theta}_3 \\ \dot{\theta}_4 \end{bmatrix} \quad (4)$$

3. System Modeling using System Identification:

The data for system identification is obtained by actuating one of the wheels and recording the encoder values of all the four wheels. It is to be noted that in real time, the wheel opposite to that of the actuating wheel tends to move but incorporating these coupling effects in the dynamic model using Euler-Lagrange equation is a tedious and complex task. Further, the inclusion of various other factors such as wear and tear of the rubber wheels, friction in bearings, aging effects of the motors in the dynamic model is difficult. Therefore, in this paper, the mathematical model is obtained using system identification tool. The output data considered in the development of the mathematical model overcomes all the above mentioned effects and hence the model obtained using this technique gives a better approximation of the real time data.

Figure 3 shows the fabricated four-wheeled mobile robot with omnidirectional wheels. As mentioned earlier, the data for system identification is obtained by actuating one of the wheels and the encoder values of all the four wheels are recorded. This results in sixteen pairs of input-output data. Thus, the data obtained from wheels other than the actuated wheel gives the coupling effect of the actuated wheel with the corresponding

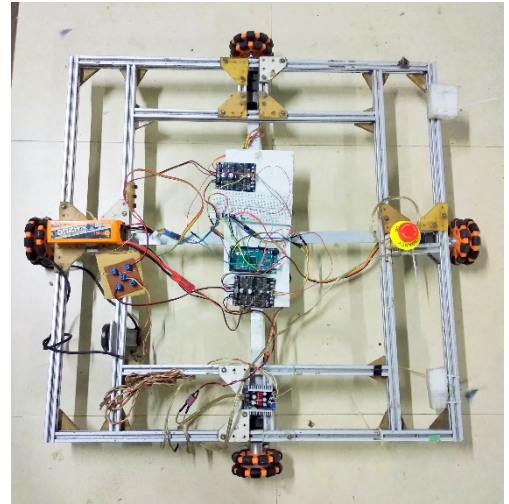


Figure 3. Fabricated four wheeled mobile base.

unactuated wheels. Figure 3 shows the plot of the step responses of the sixteen transfer functions obtained using system identification technique. To obtain the state space model from the transfer function model, an approximation is made wherein a slight tradeoff is made on the transient time but no tradeoff is made on the steady state gain of the obtained model. The effect of the aforementioned assumption is shown in figure 4. It is clear from the figure that there is no deviation between the step response of the transfer function (TF) model and the state space model (SS) of the leading diagonal elements and for other elements, a slight increase in the transient period is observed but the steady state gain remains unaltered.

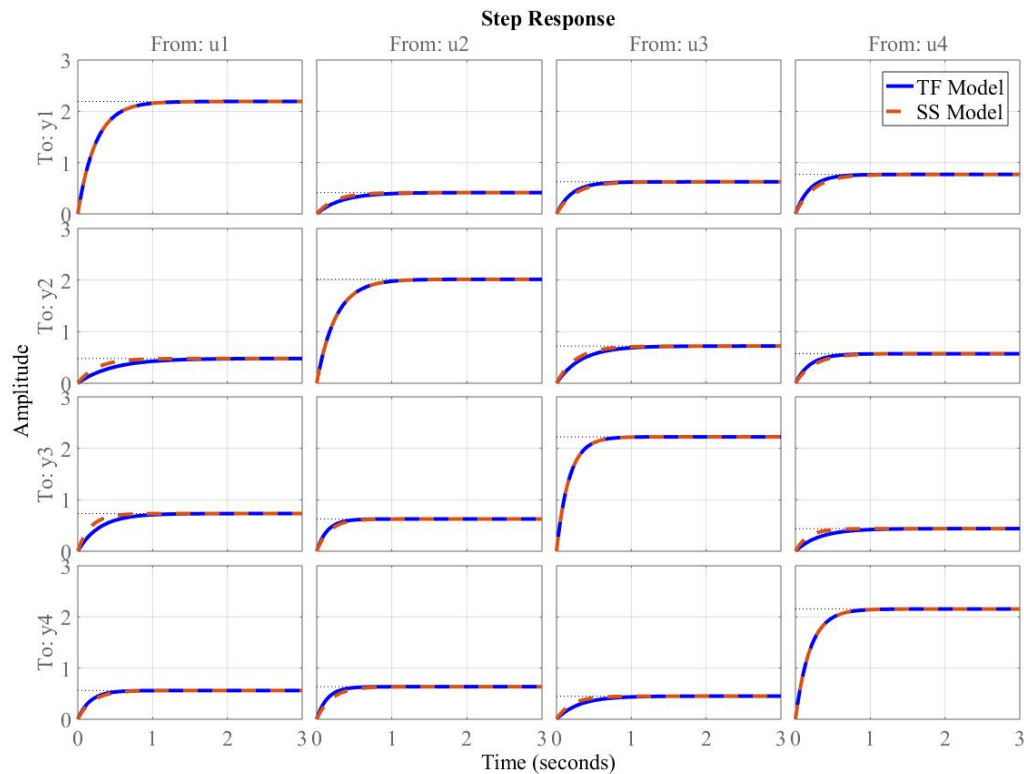
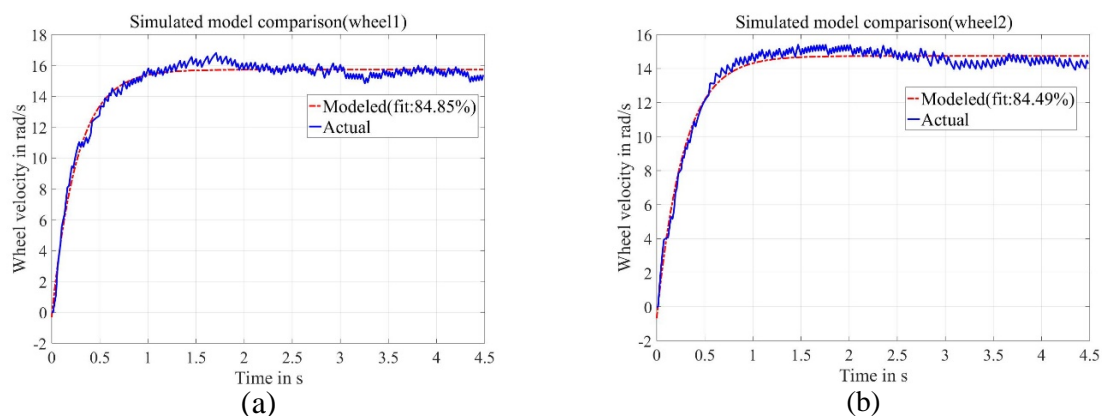


Figure 4. Step response of the transfer function model.

The modified system model is further validated using a different input-output data set. It is to be noted that all the data considered are obtained by operating the actuator at various voltages within the linear operating range. Figure 5a-5d shows the validation results of real time data and the SS model.



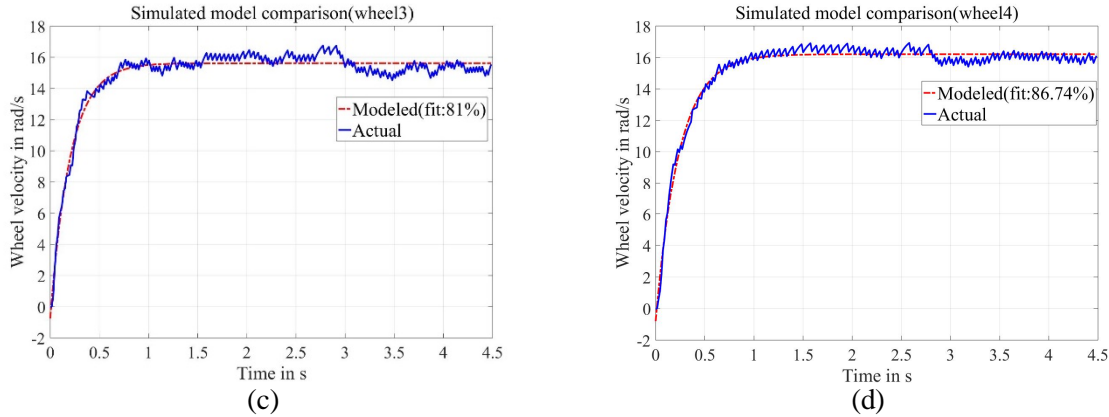


Figure 5. Velocity profile of Wheels

The validation is shown for the four diagonal transfer functions that correspond to the input-output data of the actuated wheel. The validation gives a satisfactory fit of more than 80% in all the cases and can further be improved by the using high resolution encoders and high sampling rate.

The corresponding state space model is given by:

$$\begin{aligned}\dot{X} &= AX + BU \\ Y &= CX + DU\end{aligned}$$

where,

$X = [\theta_1 \ \theta_2 \ \theta_3 \ \theta_4]^T$ is the state vector, U is the input vector; Y is the output vector;

A is the state transition matrix given by

$$A = \begin{bmatrix} -4.1462 & 0 & 0 & 0 \\ 0 & -3.9620 & 0 & 0 \\ 0 & 0 & -5.9390 & 0 \\ 0 & 0 & 0 & -5.1170 \end{bmatrix} \quad B = \begin{bmatrix} 9.0880 & 1.7220 & 2.5900 & 3.1890 \\ 1.9020 & 7.9830 & 2.8540 & 2.2850 \\ 4.3450 & 3.7160 & 13.200 & 2.6070 \\ 2.8730 & 3.2550 & 2.3100 & 11.030 \end{bmatrix}$$

$$C = \begin{bmatrix} 1 & 0 & 0 & 0 \\ 0 & 1 & 0 & 0 \\ 0 & 0 & 1 & 0 \\ 0 & 0 & 0 & 1 \end{bmatrix} \quad D = \begin{bmatrix} 0 & 0 & 0 & 0 \\ 0 & 0 & 0 & 0 \\ 0 & 0 & 0 & 0 \\ 0 & 0 & 0 & 0 \end{bmatrix}$$

4. Controller Design:

Figure 6 shows the controller block diagram of mobile robot. The trajectory tracking is carried out on the state-space model stated earlier using the optimal LQT controller and the results are compared with the conventional PID controller.

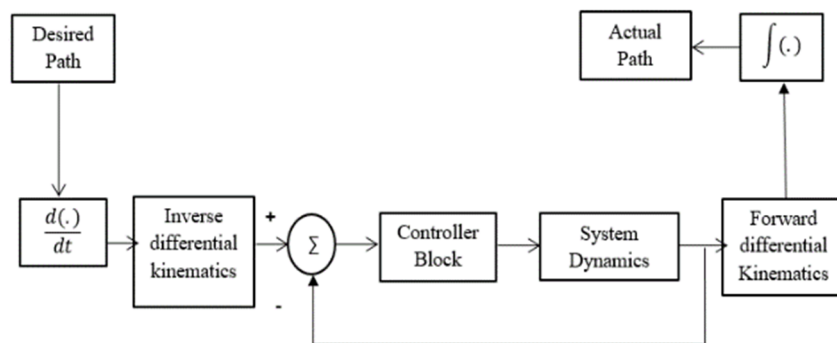


Figure 6. Controller Block diagram

4.1 LQR Controller design:

In the case of Linear quadratic tracking , the state X of a linear system $\dot{X} = AX + BU$ is to be driven to the desired set point with optimum control.

The performance index is given by: $J = \frac{1}{2} [X(t_f) - r(t_f)]^T F [X(t_f) - r(t_f)] + \frac{1}{2} \int_{t_0}^{t_f} \{ [X(t) - r(t)]^T Q [X(t) - r(t)] + U^T(t) R U(t) \} dt$

Here,

Matrix	Nature	Order
F, Q	Positive semi definite matrix	Number of states of the system
R	Positive definite matrix	Number of inputs to the system

The Hamiltonian is given by

$$H(X(t), U(t), \lambda(t), t) = \frac{1}{2} \{ [X(t) - r(t)]^T Q [X(t) - r(t)] + U^T(t) R U(t) + \lambda(t)^T (AX(t) + BU(t)) \}$$

Here, $X(t)$ and $\lambda(t)$ are state and Co-state variable

Necessary conditions for optimal control are

$$\dot{X}(t)^* = \frac{\partial H}{\partial \lambda} = AX(t) + BU(t); \quad \dot{\lambda}(t)^* = -\frac{\partial H}{\partial X} = -QX(t) - A^T \lambda(t) + Qr(t); \quad \frac{\partial H}{\partial U} = 0 = RU + B^T \lambda(t);$$

This gives the optimal control law as:

$$U^* = -R^{-1} B^T P X(t) - R^{-1} B^T S = KX(t) + V$$

where P and S can be found by using the following algebraic Riccati equations:

$$PA + A^T P - PBR^{-1} B^T P + Q = 0; \quad A^T S - PBR^{-1} B^T S + Qr(t) = 0$$

The above LQT controller is used for the trajectory tracking and the results are compared with the PI controller.

4.2 PID Controller design:

The PID control law is given by

$$u(k) = K_p e(k) + K_i T_s \sum_{i=1}^k e(i) + \frac{K_d}{T_s} \Delta e(k)$$

In this work, PI controller is used since the derivative term improves the stability of the system but increase the transient time period which in turn affects the tracking performance of the mobile robot. The parameters (K_p and K_i) of the PI controller are obtained using Auto tuning in MATLAB and are listed in the table 1.

Table 1. PID parameters.

	I	II	III	IV
K_p	0.509	0.526	0.502	0.480
K_i	8.414	7.392	12.258	9.782

5. Results

Figure 7 shows the voltage profile of all the four motors during the trajectory tracking of a rectangular trajectory using the PI and LQT controllers. It can be noted that in PI controller, whenever there is a step change in supply voltage, the actuator exhibits oscillatory response initially and then settles down.

This oscillatory response introduces tracking error but in the case of LQR controller no such oscillations are observed after the first overshoot.

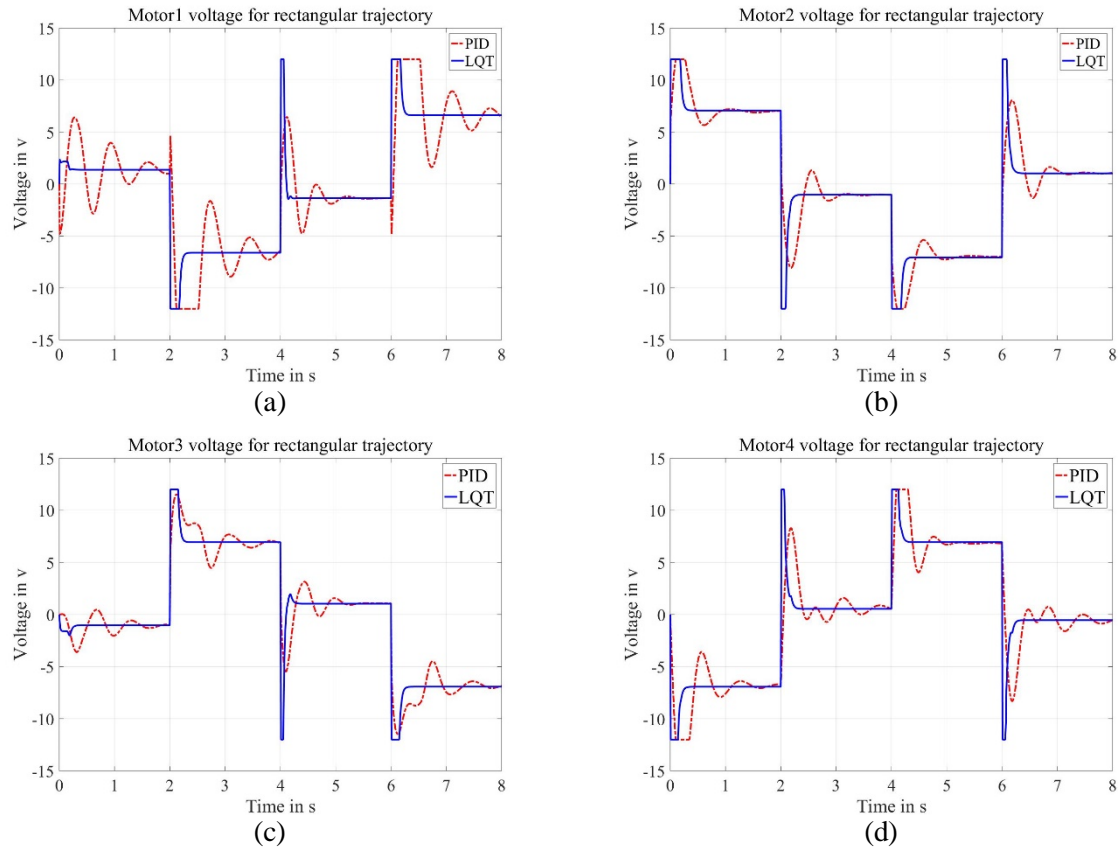


Figure 7. Voltage profile for rectangular trajectory in PI and LQT controller.

Thus, it is clear that in the case of LQT there is a small amount of error due to the overshoot but the overall tracking error is less in the case of LQT than that of PI controller. Table 2 below gives a quantitative measure of the average voltages consumed by all the four motors in the case of rectangular trajectory for both LQT and PID controllers.

Table 2. Average voltage of all the four actuators.

	U1(volts)	U2 (volts)	U3 (volts)	U4 (volts)
PI	4.6748	4.7455	4.3654	4.3804
LQT	4.3406	4.5448	4.3003	4.1543

This clearly shows the power consumed in the case of LQT is less compared to that of the PI controller. Figure 8 compares the linear velocities in X and Y directions for rectangular and circular trajectories. It can be noted that oscillations are observed in the case of PID control and is more prevalent during step changes as observed in figure 7 whereas LQR has comparatively smoother velocity profile for both rectangular and circular trajectories. Figure 9 shows the position of the robot in global frame for both the trajectories. It is clear from the figure that LQT has less tracking error than PI. This is mainly due to oscillations in the case of PI whenever there is a step change whereas in the case of LQT, oscillations are damped out after the primary overshoot.

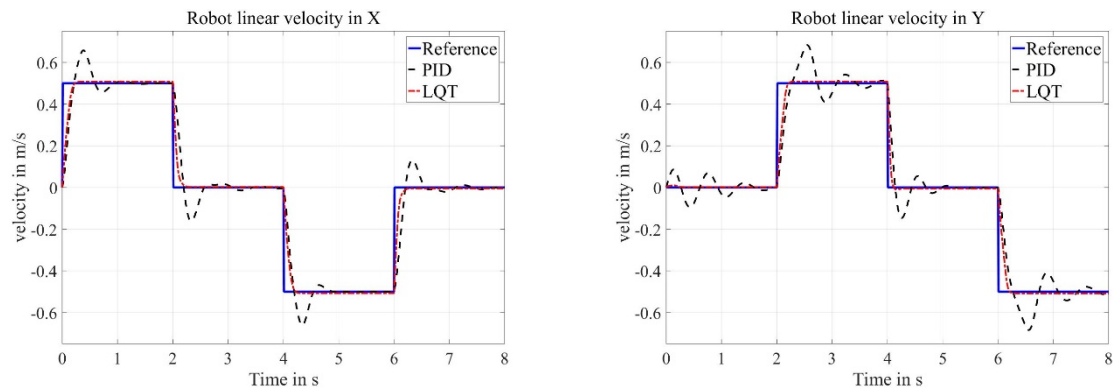
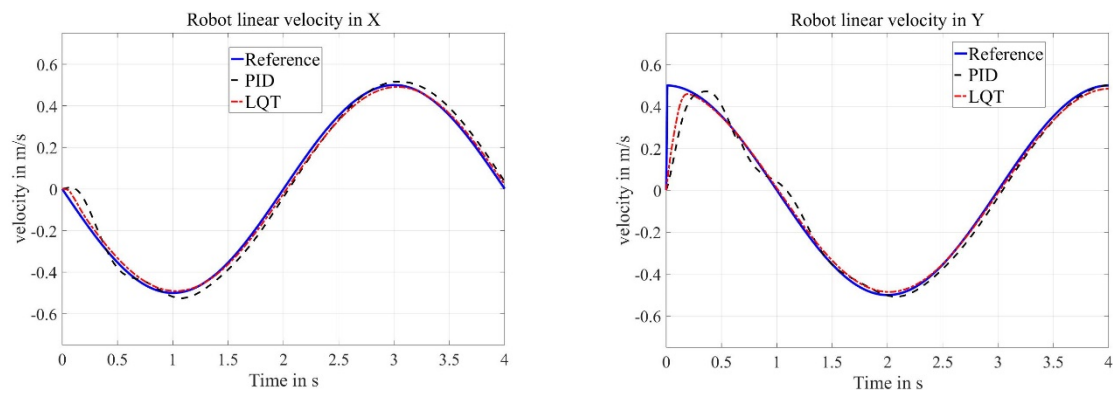
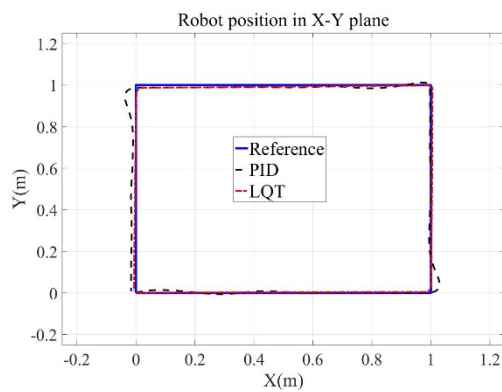
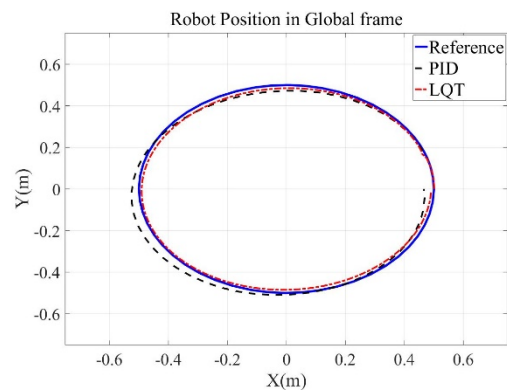
**Figure 8a.** Linear velocities of the robot for rectangular trajectory.**Figure 8b.** Linear velocities of the robot for circular trajectory.**Figure 9a.** Rectangular Trajectory**Figure 9b.** Circular Trajectory**Figure 9.** Robot position in global frame.

Table 3 and Table 4 quantifies the tracking error and gives a comparative result of PID tracking and Linear quadratic tracking. It is clear from the all these results that LQT is not only better than PID, but it gives near optimal result with very less tracking error.

Table 3. Tracking Error.

Standard Deviation		PID	LQT
Rectangular Trajectory	σ_x	0.0232	0.0167
	σ_y	0.0195	0.0192

Circular Trajectory	σ_x	0.0831	0.0177
	σ_y	0.0767	0.0239

6. Conclusion

- System identification technique is used for system modeling in this paper.
- The resulting system model accounts for various factors such as aging effects of the motor, friction between the wheel and the ground, bearing friction, mounting errors in gears, power loss due to shaft axis misalignment and so on. Thus the obtained model gives a better fit to the real time results.
- Trajectory tracking of rectangular and circular trajectories is performed using PI and LQT controller. It is found that LQR gives better tracking and consumes less energy.
- Further, the tracking can be done for eight shaped trajectories, and can be implemented on real time hardware. Design of a robust controller shall be carried out so that better tracking is obtained irrespective of disturbances.

References

- [1] Zhou K, Ebenhofer G, Eitzinger C, Zimmermann U, Walter C, Saenz J, Castaño L P, Hernández MAF and Oriol J N 2014. Mobile manipulator is coming to aerospace manufacturing industry. In *Robotic and Sensors Environments (ROSE)*, IEEE
- [2] Ortigoza R S, Marcelino Aranda M, Ortigoza G S, Guzman V M H, Molina-Vilchis, M A, Saldana-Gonzalez G, Herrera-Lozada, J C and Olguin-Carbajal M, 2012. Wheeled mobile robots: a review. *IEEE Latin America Transactions*, **10(6)** 2209-17
- [3] De Wit, C C and Sordalen O J 1992 Exponential stabilization of mobile robots with nonholonomic constraints. *IEEE Transactions on Automatic Control*, **37(11)** 1791-97.
- [4] Morin P and Samson C 2006 Trajectory tracking for nonholonomic vehicles In *Robot Motion and Control* Springer, London. 3-23
- [5] Choi Jong-Suk and Byung Kook Kim 2001 Near-time-optimal trajectory planning for wheeled mobile robots with translational and rotational sections *IEEE Transactions on Robotics and Automation* **17** 85-90.
- [6] La H T 1979 Omnidirectional Vehicle. U.S.Patent #4237990
- [7] Carlisle B 1983 An omni-directional mobile robot in *Developments in Robotics*, ed. B. Rooks, Kempston, UK: IFS. 79-87
- [8] Pin F G and Killough S M 1994 A new family of omnidirectional and holonomic wheeled platforms for mobile robots *IEEE transactions on robotics and automation* **10(4)** 480-89
- [9] Ferrière, L. and Raucourt, B., 1998, May. ROLLMOBS, a new universal wheel concept *Robotics and Automation, 1998. Proceedings. 1998 IEEE International Conf.* **3** 1877-82
- [10] West, Mark, and Haruhiko Asada 1995 Design and control of ball wheel omnidirectional vehicles In *Robotics and Automation Proceedings 1995 IEEE International Conf.* **2**, pp. 1931-38
- [11] Yiqing H Xiaofeng L Panpan W Lisheng W and Ming J 2017 Mixed fuzzy sliding mode three-dimensional trajectory tracking control for a wheeled mobile robot *Automation Youth Academic Annual Conference of Chinese Association* 5-9
- [12] Chwa D 2010 Tracking control of differential-drive wheeled mobile robots using a backstepping-like feedback linearization *IEEE Transactions on Systems, Man, and Cybernetics-Part A: Systems and Humans* **40(6)** 1285-95.
- [13] Xin L Wang Q She J and Li Y 2016 Robust adaptive tracking control of wheeled mobile robot. *Robotics and Autonomous Systems* **78** 36-48
- [14] Goswami N K and Padhy P K 2018 Sliding mode controller design for trajectory tracking of a non-holonomic mobile robot with disturbance. *Computers & Electrical Engineering* **72** 307-23